

## VOLTAGE VARIATION IN HIGH EFFICIENCY MOTORS: A TECHNICAL AND COMPUTATIONAL APPROACH

LAURO CORREA, JONATHAN M. TABORA, MARIA E. DE LIMA TOSTES, EDSON O. DE MATOS, UBIRATAN HOLANDA BEZERRA, CARMINDA C.M DE M. CARVALHO

*Centro de Excelência em Eficiência Energética da Amazônia  
Belém do Pará, Brasil*

[lauro0junior@gmail.com](mailto:lauro0junior@gmail.com), [jonathan\\_mt24@hotmail.com](mailto:jonathan_mt24@hotmail.com), [tostes@ufpa.br](mailto:tostes@ufpa.br),  
[ortiz@ufpa.br](mailto:ortiz@ufpa.br)

**Abstract**— Voltage variation is a silent enemy in electrical systems and with considerable effects on electric motors. In this work, technical experiments were carried out to evaluate the impact of this disturbance in electric motors classes IE2, IE3 and IE4, then computational simulations were carried out using genetic algorithms to predict the temperature of the analyzed motors. The results showed how the voltage variation produces deviations in consumption and temperature, while excellent temperature approximations were obtained by computational techniques.

**Keywords**— Efficiency classes, temperature, voltage variation, line-start permanent magnet motor, genetic algorithms

**Resumo**— A variação de tensão é um inimigo silencioso em sistemas elétricos e com efeitos consideráveis em motores elétricos. Neste trabalho foram realizados experimentos técnicos para avaliar o impacto desta perturbação em motores elétricos classes IE2, IE3 e IE4, em seguida foram realizadas simulações computacionais utilizando algoritmos genéticos para prever a temperatura dos motores analisados. Os resultados mostraram como a variação de tensão produz desvios de consumo e temperatura, enquanto excelentes aproximações de temperatura foram obtidas por técnicas computacionais.

**Palavras-chave**— Classes de Eficiência, temperatura, variação de tensão, motor de ímãs permanentes, algoritmos genéticos

### 1 Introduction

Electric motors represent the main load in industries, due to which special interest has been presented in the optimization of these rotating electrical machines. The main improvements lie not only in the materials, but also in the design, in addition to the introduction of new technologies such as permanent magnets in the rotor or the synchronous reluctance motor, etc.

However, despite improvements in electric motors, which make them more tolerant to disturbances present in electrical systems, their performance continues to suffer in the presence of voltage harmonics, voltage unbalance and voltage variation, the latter a silent enemy mainly in countries whose motor matrix is made up of motors imported from different countries and regions, an example of the above is the Central American region, made up of seven countries.

In the context of power quality, and according to the IEEE Std 1159 [1], voltage variation and voltage imbalance are defined as:

58  
*“Long-duration root-mean-square (rms) variation: A variation of the rms value of the voltage or current from the nominal for a time greater than 1 min. The term is usually further described using a modifier indicating the magnitude of a voltage variation (e.g., undervoltage, overvoltage, voltage interruption).”*

The voltage variation can result in the variation of consumption, efficiency, and power factor; however, these parameters are not usually considered at the time of replacement, the degree of deviation will depend on the percentage of overvoltage or undervoltage existing in the electric motor input.

Computational intelligence becomes a very useful tool in the industry, its multiple applications in prediction allow not only better monitoring, but also the guarantee of a longer life from programmed maintenance or in the presence of abnormal operation.

Different works have analyzed performance and losses in electrical motors through thermography and computational methods [2]–[11]. In [12], it was presented the result of a statistical analysis related to the thermal behavior and life expectancy of three-phase induction motors under non sinusoidal supply, considering the random nature voltage variation caused by dynamic operation of the electrical power system.

In [12], [13] and [14], the authors presented a comparative study on high-efficiency, premium and super-premium electric motor when subjected to voltage harmonic distortion and unbalance. The results presented in [12], [15] showed that there are correlations among the harmonic component and motor's temperature and that these correlations vary depending of the motor. And, in [14], the results depicted that voltage unbalance might significantly affect the motors' temperature and harmonic content.

In this sense, this paper presents a model that explains how the harmonic voltages affects the motors` frame temperature using regression techniques.

In this sense, this article presents an experimental evaluation of the impact of voltage variation in electric motors classes IE2, IE3 and IE4, as well as computational intelligence through genetic algorithms to predict the increase in temperature in electric motors with the presence of voltage variation.

### 3. Methodology

#### 3.1 Methodology Process

The experiment bench was powered using the three phase AC source model FCATHQ brand Supplier, capable of generating pure sine voltage waveforms with programmable amplitude.

To measure and record tension, current, power factor and power data was used the model PW3198-90 A class power analyzer brand HIOKY.

To gather the temperature data were used the thermographic camera model T620 brand FLIR. During the experiments frontal and lateral photos were taken at two-minute intervals.

In order to simulate load at the motors shaft an electromagnetic brake were used. First, during the experiments at rated voltage supply, the brake was adjusted so the motors reached their rated currents. During the next experiments, at voltage supply deviation, the brake was adjusted to reach the same torque observed at rated voltage. The Experiment bench was assembled as shown on figure 3.1.1.

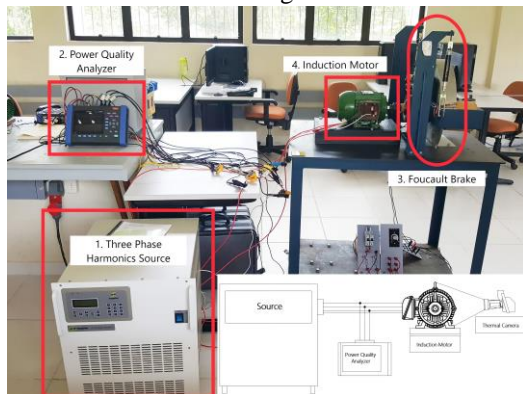


Figure 1. – Test bench

The motor parameters provided by the manufacturer are shown in Table 1. The experiments lasted for one hour and ten minutes and through all its duration the magnetic brake was regulated to maintain the nominal parameters (rated line current).

Table 1 – Motor Parameters

	Motor Efficiency Class		
	IE2	IE3	IE4
Tecnology	SCIM	SCIM	LSPM
Power	1 cv	1 cv	1 cv
Voltage	220 V/380 V	220 V/380 V	220 V/380 V
RPM	1730	1725	1800
Torque	4,12	4,13	3,96
Current	2,98/1,73	2,91/1,68	3,08/1,78
Efficiency	82,60	82,6	87,4
Power Factor	0,80	0,82	0,73

Next, the photos were submitted to data processing through FLIR's camera software then a model (discussed latter) was generated for each motor heating curve using a genetic algorithm-based curve fitting program. A flow chart for the methodology process is showed in fig. 2

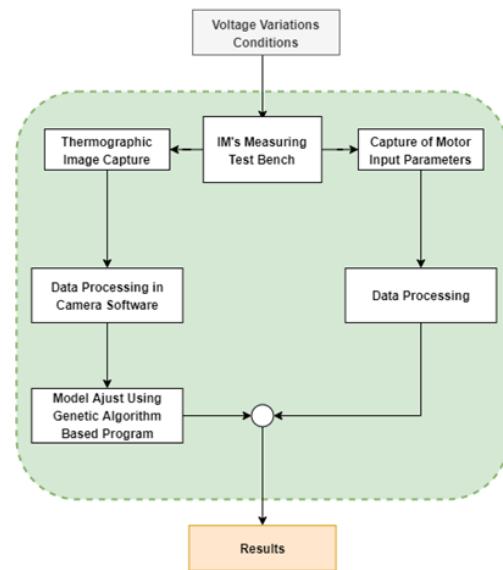


Figure 2 - Methodology process flow chart

#### 3.2 Model

Assuming that losses in each test produces a constant amount of heat through the experiment and the function (1) from [1, pg. 98], an approximation for the heating curve of an sphere, the several constants are reduced to three, as seen in function (2), and the new model is used to approximate the heating process. The new constants values are found using a genetic algorithm.

$a$  – Radius

$D$  – Diffusion Constant

$T$  – Temperature

$T_1$  – Heat Source Temperature

$T_0$  – Initial Temperature

$t$  – Time

$$T(0, t) \approx T_1 - 2(T_1 - T_0)e^{-D(\pi/a)^2 t} \quad (1)$$

$C_1, C_2$  – Constants Dependent of Ambient and Heating Conditions  
 $k$  – Constant Dependent of Motor Characteristics  
 $T$  – Temperature  
 $t$  – Time

$$T(t) \approx C_1 - C_2 e^{-t/k} \quad (2)$$

Through this model, the steady state for the motor temperature can be better estimated than, for example, a polynomial curve fitting, since the polynomial fitting diverges for values not on the measured data range and the proposed model represents better the phenomenon.

### 3.3 Curve fitting algorithm

Using a genetic algorithm, the model presented in the previous section is fitted to the measured temperature data of each experiment. The algorithm works by taking the following steps:

An initial generation, consisted of individuals with three genes, each representing one of the model constants ( $C_1$ ,  $C_2$  or  $k$ ), is randomly generated.

Then a loop, that lasts for a set number of iterations, is started, where, based on the mean square error in relation to the measured temperature, the best individuals are selected to make up the next generation through the mating process.

When the loop ends, the best individual is chosen as the best model for the measured temperature.

The algorithm's flowchart is showed in fig. 3

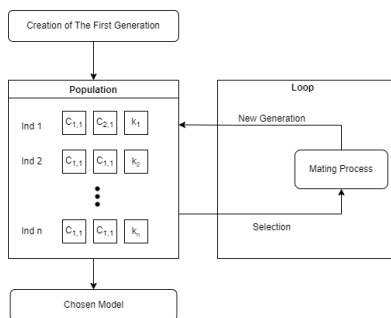


Figure 3 – Genetic Algorithm Flow Chart

## 4. Results

### 4.1 Line Current

It can be seen in tables 2 and 3 how the deviation of voltage feeding from the rated value causes a higher value for line current in IE2 and IE3 class motors, both on undervoltage and

overvoltage, while only overvoltage causes an increased current for IE4 motor, however, with much higher values, reaching currents 13% higher than the rated value. The current through the experiments is shown in figs. 4, 5 and 6

Motor	Mean Line Current (A)				
	1.00pu	0.90 pu	0.95 pu	1.05 pu	1.10 pu
IE2	2.96	3.09	2.98	2.99	3.05
IE3	2.89	3.00	2.92	2.90	2.98
IE4	3.06	3.00	3.05	3.19	3.47

Table 2 – Mean Line Current Amperes

Motor	Base Value	Mean Line Current (%)			
		1.00pu	0.90 pu	0.95 pu	1.05 pu
IE2		+ 4.56%	+ 0.73 %	+ 1.04 %	+ 3.07%
IE3		+ 3.86%	+ 1.08%	+ 0.27%	+ 3.00%
IE4		- 2.00%	- 0.41%	+ 4.26%	+13.17%

Table 3 – Mean Line Current Percentage

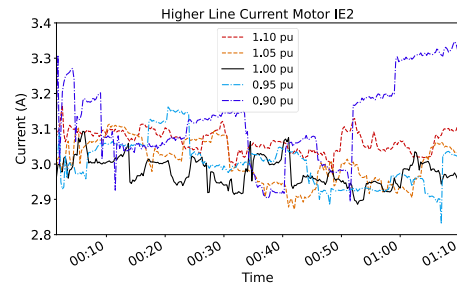


Figure 4 – Line Current IE2

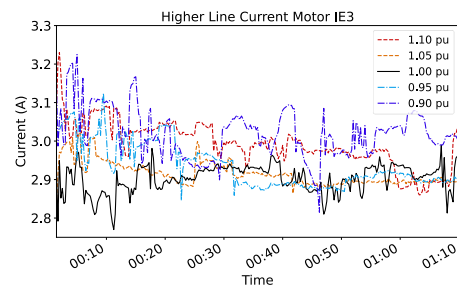


Figure 5 – Line Current IE3

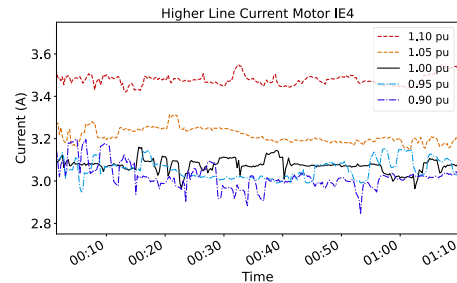


Figure 6 – Line Current IE4

### 4.2 Energy Consumption

The consumption for the IE2, IE3 and IE4 class motors is presented in figures 7, 9 and 11 respectively. It is perceived that the consumption

of IE2 and IE3 motors is slightly increased for overvoltage and undervoltage conditions, with exception of a small decrease for the 0.95 p.u. voltage magnitude, while the IE4 motor's consumption is proportional to the input voltage. To better see the variation in each motor, the motor percentage increase in consumption is presented in figures 8, 10 and 12, with relation to the nominal voltage experiment, it can be seen how the IE2 and IE3 Class motors present similar responses, different from the IE4 Class motor whose consumption varies according to the voltage magnitude.

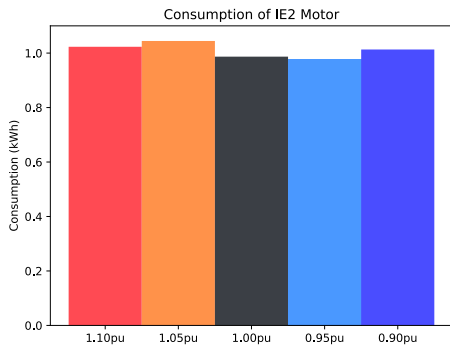


Figure 7 – IE2 Motor Energy Consumption

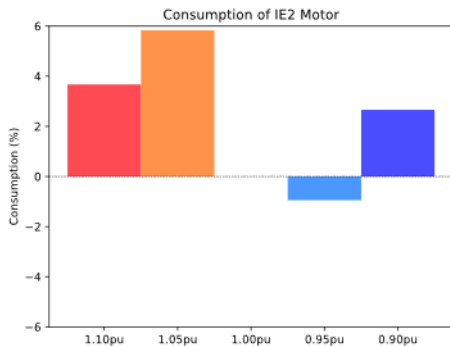


Figure 8 – IE2 Motor Percentage of Consumption Increase

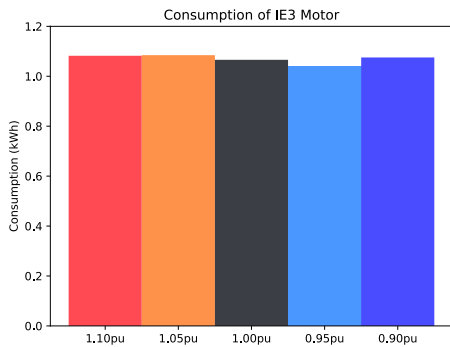


Figure 9 – IE3 Motor Energy Consumption

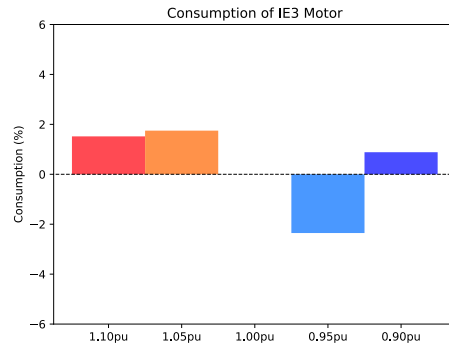


Figure 10 – IE3 Motor Percentage of Consumption Increase

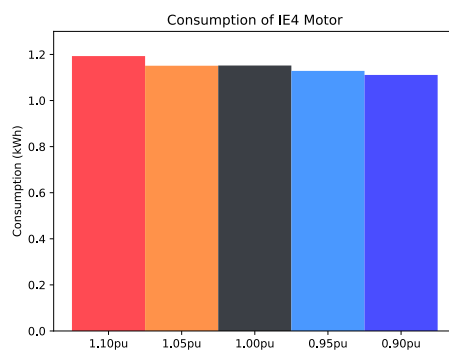


Figure 11 – IE4 Motor Energy Consumption

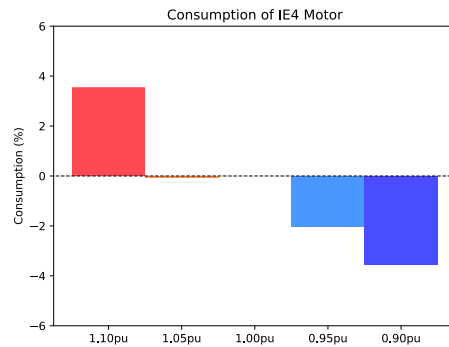


Figure 12 – IE4 Motor Percentage of Consumption Increase

### 4.3 Temperature Analysis

The temperature increase with each voltage variation condition is presented in figures 13-18. Each point in the graph shows the highest temperature in that instant for each motor region (side or front). It can be

It can be observed how the temperature varies according to every electric motor class, in the case of the IE2 and IE4 class motors, the 1.10 p.u. voltage condition resulted in higher temperatures, different to the IE3 Class motor, who presented higher temperatures for the 0.90

p.u. conditions. This results will be validated to computational models.

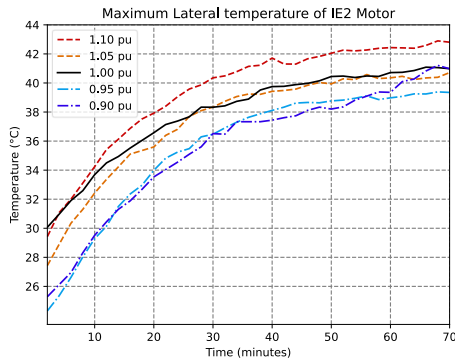


Figure 13 – IE2 Lateral Temperature

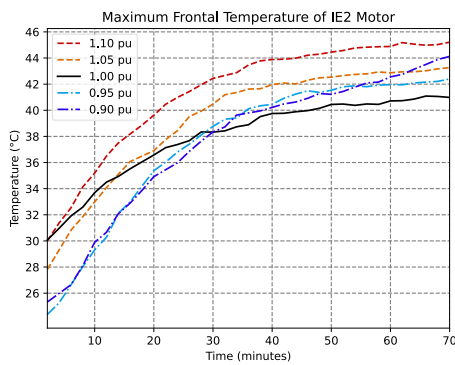


Figure 14 – IE2 Frontal Temperature

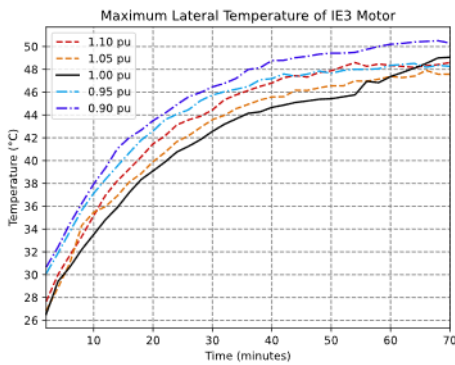


Figure 15 – IE3 Lateral Temperature

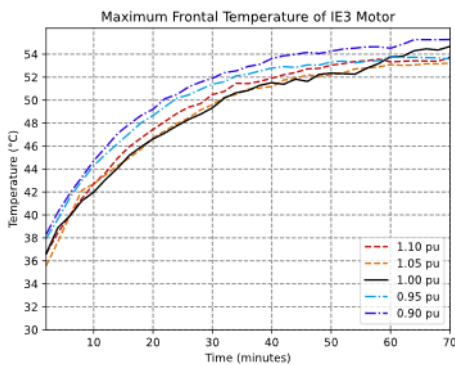


Figure 16 – IE3 Frontal temperature

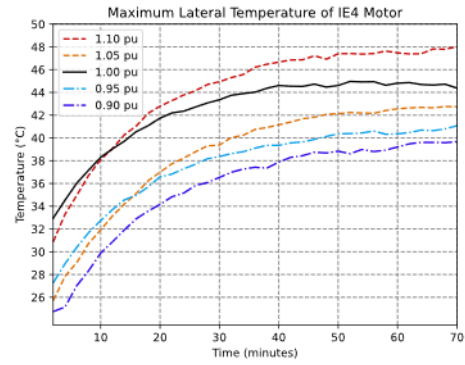


Figure 17 – IE4 Lateral Temperature

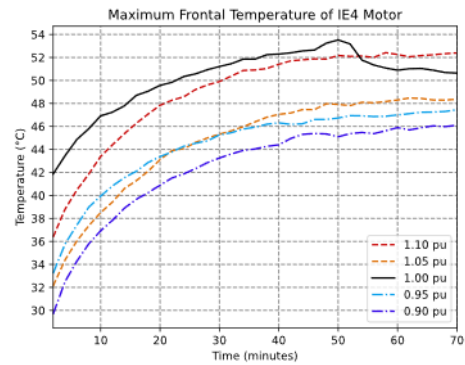


Figure 18 – IE4 Frontal temperature

Based on the temperature measurements, genetic algorithm was used to obtain the temperature models. The coefficient vector ( $C_1$ ,  $C_2$  and  $k$ ), correlation coefficient and mean square error from each model are shown in tables 4, 5 and 6. the heating curves generated from the models are shown in figures 19-24.

IE2 Temperature Models

	Lateral			Frontal		
	Coefficient Vector (C1, C2, k)	Correlation coefficient	Mean Square Error	Coefficient Vector (C1, C2, k)	Correlation coefficient	Mean Square Error
1.10 pu	[42.95, 15.15, 17.69]	0.998	0.022	[45.58, 17.82, 17.85]	0.020	0.998
1.05 pu	[40.88, 15.11, 17.22]	0.997	0.032	[43.76, 18.06, 18.56]	0.075	0.996
1.00pu	[41.51, 12.62, 21.50]	0.998	0.017	[45.24, 15.25, 22.04]	0.026	0.998
0.95 pu	[39.82, 18.14, 17.75]	0.997	0.046	[43.28, 22.17, 19.81]	0.135	0.995
0.90 pu	[40.13, 16.93, 21.31]	0.993	0.166	[44.42, 21.74, 24.76]	0.343	0.978

Table 4 – IE2 Temperature Models

IE3 Temperature Models

	Lateral			Frontal		
	Coefficient Vector (C1, C2, k)	Correlation coefficient	Mean Square Error	Coefficient Vector (C1, C2, k)	Correlation coefficient	Mean Square Error
1.10 pu	[49.24, 24.40, 17.70]	0.998	0.046	[54.28, 19.72, 18.71]	0.021	0.999
1.05 pu	[48.21, 23.36, 18.70]	0.996	0.112	[53.82, 19.41, 19.46]	0.091	0.995
1.00pu	[47.56, 22.93, 19.91]	0.982	0.562	[54.03, 18.90, 21.12]	0.260	0.987
0.95 pu	[48.76, 21.64, 15.81]	0.998	0.028	[53.98, 18.41, 15.63]	0.016	0.999
0.90 pu	[50.78, 22.73, 17.57]	0.998	0.036	[55.48, 19.10, 17.61]	0.016	0.999

Table 5 – IE3 Temperature Models

IE4 Temperature Models

	Lateral			Frontal		
	Coefficient Vector (C1, C2, k)	Correlation coefficient	Mean Square Error	Coefficient Vector (C1, C2, k)	Correlation coefficient	Mean Square Error
1.10 pu	[48.00, 19.13, 15.63]	0.998	0.027	[52.57, 18.23, 14.99]	0.020	0.998
1.05 pu	[43.14, 19.59, 17.40]	0.999	0.013	[48.91, 18.31, 17.92]	0.025	0.998
1.00pu	[44.99, 13.97, 13.80]	0.996	0.031	[53.17, 12.52, 15.82]	1.005	0.886
0.95 pu	[40.91, 15.18, 16.56]	0.998	0.020	[47.19, 15.32, 14.17]	0.0457	0.996
0.90 pu	[39.86, 17.65, 17.85]	0.997	0.048	[46.17, 17.69, 16.27]	0.057	0.996

Table 6 – IE4 Temperature Models

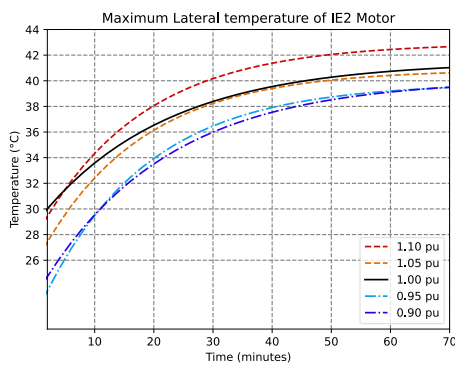


Figure 19 - IE2 Lateral Temperature Model

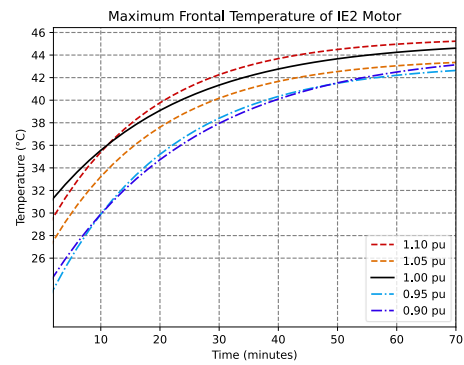


Figure 20 - IE2 Lateral Temperature Model

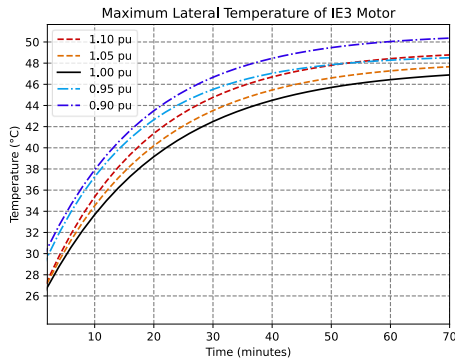


Figure 21 – IE3 Lateral Temperature Model

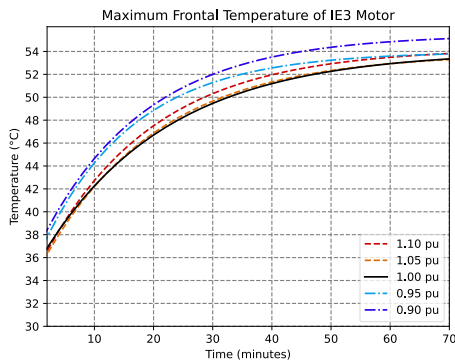


Figure 22 – IE3 Frontal Temperature Model

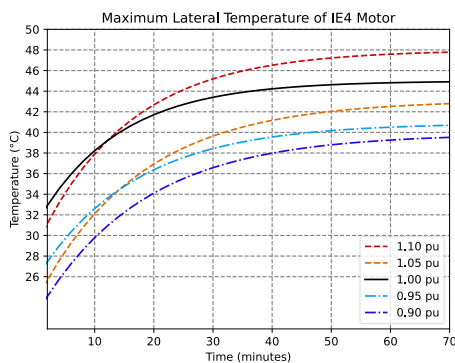


Figure 23 – IE4 Lateral Temperature Model

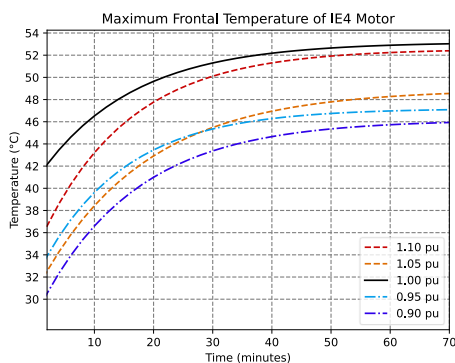


Figure 24 – IE4 frontal Temperature Model

Figures 25 and 26 presents the variation from the motor's initial temperature to the steady state temperature based on the model. It can be seen how the temperature variation increases when the voltage shifts from its rated value on IE2 and IE4 class motors, while the IE3 class motor is less affected.

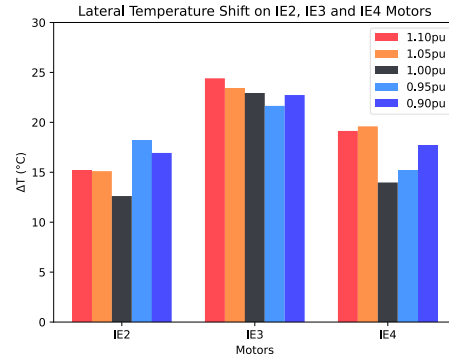


Figure 25– Lateral Temperature Variation for the Three Motors

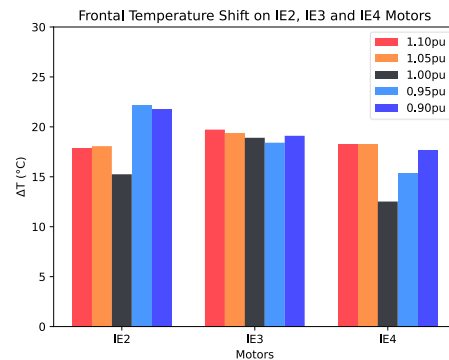


Figure 26 – Frontal Temperature Variation for the Three Motors

#### 4. Conclusions

Given the evolution of electric motors, the impact of disturbances on new technologies must be analyzed. A disturbance present in the electrical systems is the variation of voltage, product of the different levels of voltage in the multiple countries. In this sense, this work analyzed different percentages of voltage variation in electric motors classes IE2, IE3 and IE4. It was observed how the voltage variation results in temperature and consumption deviations in relation to its nominal value, for which special care must be given by the engineers, mainly in the economic calculation for the substitution. Finally, genetic algorithms were used to estimate the temperature increase in the presence of voltage variation, great approximations were obtained with the presented technique.

#### 5. References

- [1] "IEEE Recommended Practice for Monitoring Electric Power Quality," *IEEE Std 1159-2019 (Revision of IEEE Std 1159-2009)*, pp. 1–98, Aug. 2019, doi: 10.1109/IEEESTD.2019.8796486.
- [2] B. Zöhra, M. Akar, and M. Eker, "Design of A Novel Line Start Synchronous Motor Rotor," *Electronics*, vol. 8, no. 1, Art. no. 1, Jan. 2019, doi: 10.3390/electronics8010025.
- [3] "Energies | Free Full-Text | Study on Line-Start Permanent Magnet Assistance Synchronous Reluctance Motor for Improving Efficiency and Power Factor." <https://www.mdpi.com/1996-1073/13/2/384> (accessed Dec. 06, 2020).
- [4] H. Qiu, Y. Xu, Y. Liu, J. Sun, and C. Yang, "Influence of magnetic slot wedge on the performance of 10-kV, 1000-kW permanent magnet synchronous motor," *International Transactions on Electrical Energy Systems*, vol. 30, no. 5, p. e12332, 2020, doi: <https://doi.org/10.1002/2050-7038.12332>.
- [5] E. Sarani and S. Vaez-Zadeh, "Line start permanent magnet motors with double-barrier configuration for magnet conservation and performance improvement," *IET Electric Power Applications*, vol. 11, no. 9, pp. 1656–1663, 2017, doi: 10.1049/iet-epa.2017.0086.
- [6] R. D. Paiva Jr, V. C. Silva, S. I. Nabeta, and I. E. Chabu, "Magnetic topology with axial flux concentration: a technique to improve permanent-magnet motor performance," *Journal of Microwaves, Optoelectronics and Electromagnetic Applications*, vol. 16, no. 4, pp. 881–899, Dec. 2017, doi: 10.1590/2179-10742017v16i4957.
- [7] "Novel Analytical Method for Overhang Effects in Surface-Mounted Permanent-Magnet Machines - IEEE Journals & Magazine." <https://ieeexplore.ieee.org/document/8826274> (accessed Dec. 06, 2020).
- [8] S. Saha and Y.-H. Cho, "Starting Characteristic Analysis of LSPM for Pumping System Considering Demagnetization," *undefined*, 2015. /paper/Starting-Characteristic-Analysis-of-LSPM-for-System-Saha-Cho/26294607254e76bf172d45825973f83ac4b7cbb9 (accessed Dec. 06, 2020).
- [9] S. Saha and Y.-H. Cho, "Starting Characteristic Analysis of LSPM for Pumping System Considering Demagnetization," *International Journal of Mechanical and Mechatronics Engineering*, vol. 9, no. 7, pp. 1305–1311, Jul. 2015, Accessed: Dec. 06, 2020. [Online]. Available: <https://publications.waset.org/10002153/starting-characteristic-analysis-of-lspm-for-pumping-system-considering-demagnetization>
- [10] A. Cavagnino, S. Vaschetto, L. Ferraris, Z. Gmyrek, E. B. Agamloh, and G. Bramerdorfer, "Striving for the Highest Efficiency Class With Minimal Impact for Induction Motor Manufacturers," *IEEE Transactions on Industry Applications*, vol. 56, no. 1, pp. 194–204, Jan. 2020, doi: 10.1109/TIA.2019.2949262.
- [11] F. Ghoroghchian, A. D. Aliabad, and E. Amiri, "Two-Speed Line Start Permanent Magnet Synchronous Motor With Dual Magnetic Polarity," *IEEE Transactions on Industry Applications*, vol. 54, no. 5, pp. 4268–4277, Sep. 2018, doi: 10.1109/TIA.2018.2839609.
- [12] J. Muñoz Tabora, M. E. de Lima Tostes, E. Ortiz de Matos, T. Mota Soares, and U. H. Bezerra, "Voltage Harmonic Impacts on Electric Motors: A Comparison between IE2, IE3 and IE4 Induction Motor Classes," *Energies*, vol. 13, no. 13, Art. no. 13, Jan. 2020, doi: 10.3390/en13133333.
- [13] J. M. Tabora, M. E. D. L. Tostes, E. O. De Matos, U. H. Bezerra, T. M. Soares, and B. S. De Albuquerque, "Assessing Voltage Unbalance Conditions in IE2, IE3 and IE4 Classes Induction Motors," *IEEE Access*, pp. 1–1, 2020, doi: 10.1109/ACCESS.2020.3029794.
- [14] J. M. Tabora *et al.*, "Assessing Energy Efficiency and Power Quality Impacts Due to High-Efficiency Motors Operating Under Nonideal Energy Supply," *IEEE Access*, vol. 9, pp. 121871–121882, 2021, doi: 10.1109/ACCESS.2021.3109622.
- [15] M. T. Jonathan, E. Ortiz de Matos, T. M. Soares, M. E. de L. Tostes, and J. C. Paye, "Fifth & Seventh Harmonic Effects on the Performance of IE2, IE3 & IE4 Induction Motor Classes," in *Proceedings of the 13th Latin-American Congress on Electricity Generation and Transmission - CLAGTEE 2019*, Santiago, Chile, Oct. 2019, p. 6. [Online]. Available: <http://www.clagtee2019.pucv.cl/2019/book.html>
- [16] "Ministério de Minas e Energia, "Plano Nacional de Energia 2030"." <https://www.epe.gov.br/pt/publicacoes-dados-abertos/publicacoes/Plano-Nacional-de-Energia-PNE-2030> (accessed Sep. 23, 2021).
- [17] I. Nacional, "PORTARIA INTERMINISTERIAL Nº 1, DE 29 DE JUNHO DE 2017 - Imprensa Nacional." <https://www.in.gov.br/materia> (accessed Sep. 23, 2021).
- [18] F. J. T. E. Ferreira and A. T. de Almeida, "Energy savings potential associated with stator winding connection mode change in induction motors," in *2016 XXII International Conference on Electrical Machines (ICEM)*, Sep. 2016, pp. 2775–2783. doi: 10.1109/ICELMACH.2016.7732915.
- [19] J. M. Tabora *et al.*, "Induction Motors Assessment: A Substitution Case Analysis," in *2021 14th IEEE International Conference on Industry Applications (INDUSCON)*, Aug. 2021, pp. 783–789. doi: 10.1109/INDUSCON51756.2021.9529738.
- [20] F. J. T. E. Ferreira, B. Leprettre, A. Q. Duarte, and A. T. De Almeida, "Comparison of protection requirements in IE2-, IE3-, and IE4-class motors," in *2015 IEEE International Electric Machines Drives Conference (IEMDC)*, May 2015, pp. 1874–1880. doi: 10.1109/IEMDC.2015.7409320.
- [21] S. J. Chapman and A. Laschuk, *Fundamentos de Máquinas Elétricas*, 5ª edição. AMGH, 2013.
- [22] "SOMA BD Motor." <https://bdmotor.cepel.br/> (accessed Sep. 23, 2021).
- [23] "See+." <https://www.weg.net/see+/pages/regua.jsp> (accessed Sep. 23, 2021).
- [24] P. of P. S. J. Blundell and K. M. Blundell, *Concepts in Thermal Physics*, 2nd ed. edição. Oxford; New York: Oxford University Press, USA, 2009.